Available online at www.sciencedirect.com
ScienceDirect
Tetrahedron
Tetrahedron 63 (2007) 2851–2858

Synthesis and optical/thermal properties of low molecular mass V-shaped materials based on 2,3-dicyanopyrazine

Rodrigo Cristiano,[a] Eduard Westphal,[a] Ivan H. Bechtold,[b] Adailton J. Bortoluzzi[a] and Hugo Gallardo[a,*]

[a]*Departamento de Química, Universidade Federal de Santa Catarina, 88040-900 Florianópolis, SC, Brazil*
[b]*Departamento de Física, Universidade Federal de Santa Catarina, 88040-900 Florianópolis, SC, Brazil*

Received 1 November 2006; revised 8 January 2007; accepted 22 January 2007
Available online 25 January 2007

Abstract—A novel series of luminescent low molecular mass materials containing a 2,3-dicyanopyrazine central core were synthesized through an esterification reaction between diphenol **10** and different aromatic carboxylic acids **1**–**6**, containing terminal long alkyl chains. They have a similar V-shaped geometry with lack of planarity between the two arms, confirmed by the X-ray structure of the central core. The optical and thermal properties of these compounds were evaluated. They show blue fluorescence in solution (λ_{em}^{max} 440–480 nm) with quantum fluorescence yields (Φ_F) from 0.003 to 0.1 and Stokes shifts of around 90 nm. In solid state, optical band gaps (E_g) were from 3.14 to 3.32 eV. Thin films of **11**, **13**, and **14** exhibited blue fluorescence (λ_{em}^{max} 430–456 nm), and **12**, **15**, and **16** (more bulky) displayed green fluorescence (λ_{em}^{max} 488–512 nm). Most of the materials exhibited good thermal stability, exhibiting an amorphous glassy state after melting. Transparent amorphous films were easily obtained through spin coating and characterized by AFM analysis.

1. Introduction

Organic compounds that exhibit a variety of interesting optical, electrical, photoelectrical, and magnetic properties in the solid state have found widespread use in a growing number of practical applications, including their utility as emitters in light-emitting diodes,[1] laser dyes,[2] photoconductors,[3] optical switches,[4] and optical data storage devices.[5] Low molecular mass materials that are able to form stable films are particularly interesting in such functional systems due to their well-defined molecular structures and molecular weights, and also because they can be easily purified. Among these materials and their organization states, two classes in particular have been extensively exploited: fluorescent liquid crystals,[6] as the self organizing properties of these materials can lead to defect-free layers with high carrier mobility for electroluminescence devices, and various types of amorphous molecular glass, because of their good processability, transparency, and homogeneity.[7]

Dicyanopyrazine derivatives have been synthesized and are valuable in a broad range of chemistry fields due to their applications as functional dyes, nonlinear optical materials, etc.[8] They have strong electron withdrawing ability and, despite possessing a small chromophoric system, they present strong fluorescence even in solid state.[9] In this context, our research is focused on fluorescent molecular materials containing electron deficient *N*-heterocycles that can exhibit either liquid crystalline phases[10] or a stable glassy state for opto-electronic applications.

In this paper, we report on the synthesis of a series of fluorescent 2,3-dicyanopyrazine derivatives (**11**–**16**) possessing a similar V-shaped geometry[11] with some lack of planarity, in order to achieve a mesomorphic or film forming behavior. The photophysical properties in solution and in thin film, along with the thermal behavior of these compounds, were also evaluated.

2. Results and discussion

2.1. Synthesis

Scheme 1 outlines the synthesis of the series of 2,3-dicyanopyrazine derivatives. Anisil **7** was prepared from 4-methoxybenzaldehyde through benzoin condensation followed by hydroxyl group oxidation using $CuSO_4$/pyridine. A condensation reaction of anisil **7** with diaminomaleonitrile (DAMN) in the presence of a catalytic amount of *p*-toluenesulfonic acid (*p*-TsOH) gave the 2,3-dicyanopyrazine derivative **8** in good yield (90%). An attempt to achieve methyl

Keywords: 2,3-Dicyanopyrazine; Luminescent materials; X-ray structure; Functional dyes.
* Corresponding author. Fax: +55 48 3721 6850; e-mail: hugo@qmc.ufsc.br

0040–4020/$ - see front matter © 2007 Elsevier Ltd. All rights reserved.
doi:10.1016/j.tet.2007.01.045

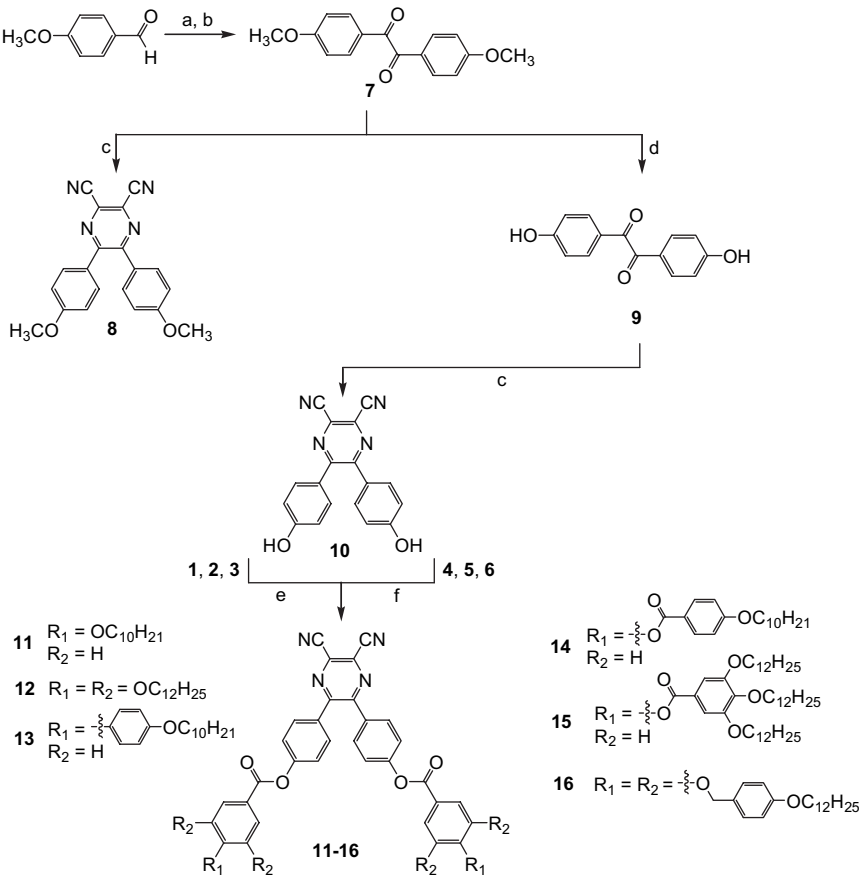

Scheme 1. Synthetic route for final compounds **11**–**16**. Conditions (yield): (a) KCN, EtOH/H_2O, reflux (38%); (b) $CuSO_4$, pyridine/H_2O, 60 °C (93%); (c) diaminomaleonitrile, $TsOH_{cat.}$, MeOH, reflux (90%); (d) $HBr_{(aq)}$, AcOH, reflux (69%); (e) (i) respective carboxylic acid (**1**, **2**, or **3**), $SOCl_2$, CH_2Cl_2, reflux (100%); (ii) TEA, CH_2Cl_2, rt (70–85%); (f) respective carboxylic acid (**4**, **5**, or **6**), DCC, $DMAP_{cat.}$, CH_2Cl_2, rt (70–85%).

group elimination was firstly carried out using BBr_3, however, this gave poor yields of compound **10**. Thus, another approach was performed, in which anisil **7** was demethylated by refluxing it in a 1:1 $HBr_{(aq)}$/acetic acid mixture. This procedure was found to be better, giving diphenol **9**, which was reacted with DAMN and *p*-$TsOH_{cat.}$ affording compound **10**. The final compounds **11**–**16** were synthesized through esterification of diphenol **10** with different, previously prepared, aromatic carboxylic acids **1**–**6** shown in Figure 1. Two approaches were used: for carboxylic acids **1**–**3** the reaction was carried out using the freshly prepared acid chloride in the presence of triethylamine in dichloromethane; and for carboxylic acids **4**–**6**, to avoid ester or benzyl ether cleavage of these acids by thionyl chloride, the esterification was performed with dicyclohexylcarbodiimide (DCC) in the presence of catalytic amount of dimethylaminopyridine (DMAP).

The structures of all the compounds were characterized by IR, ^1H, and ^{13}C NMR spectra and elemental analysis, including X-ray diffraction analysis of compound **8**.

2.2. X-ray diffraction analysis of the central core

Considering the enormous difficulty in crystallizing the final compounds **11**–**16**, the well-crystalline intermediate 2,3-dicyanopyrazine derivative **8** was crystallized and analyzed by single crystal X-ray diffraction for a better understanding of the solid state nature of the final molecules, since these materials have the same central core. Slightly yellow crystals of **8** suitable for X-ray analysis were obtained by recrystallization from methanol. The crystal structure and selected bond lengths and angles of **8** are presented in Figure 2.

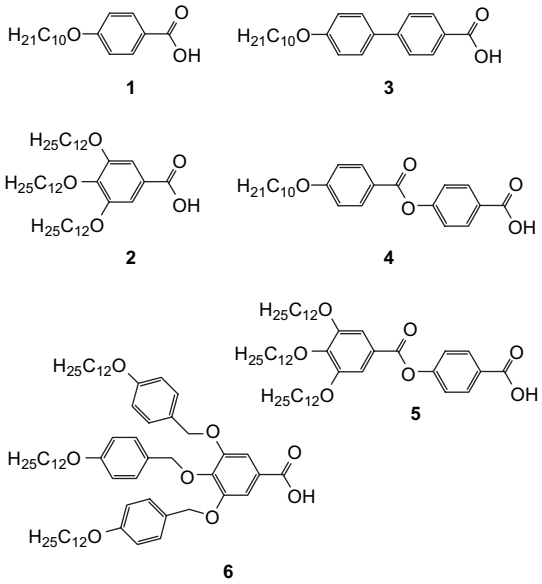

Figure 1. Carboxylic acid intermediates **1**–**6** synthesized.

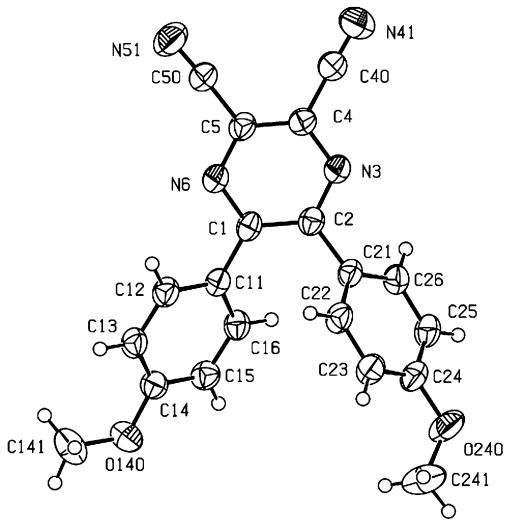

Figure 2. Molecular structure of compound **8** with atom labeling scheme. Selected bond distances and angles: C(1)–N(6) 1.341(2), C(1)–C(2) 1.434(3), C(1)–C(11) 1.475(3), C(2)–N(3) 1.335(3), C(2)–C(21) 1.480(3), N(3)–C(4) 1.345(3), C(4)–C(5) 1.386(3), C(5)–N(6) 1.341(3), C(1)–C(2)–N(3) 120.76(19), C(2)–N(3)–C(4) 117.66(18), N(3)–C(4)–C(5) 121.6(2), C(4)–C(5)–N(6) 121.45(19), C(5)–N(6)–C(1) 117.99(18), N(6)–C(1)–C(2) 120.1(2).

As shown in Figure 2, the two 4-methoxyphenyl groups connected to positions 5 and 6 of 2,3-dicyanopyrazine are twisted with respect to each other and they are not coplanar with the central pyrazine ring. The planes of both 4-methoxyphenyl rings are rotated with respect to the mean plane of the pyrazine ring by 40.39(6)° and 48.36(5)°, and with respect to each other by 48.95(6)°. The nonplanarity of this compound is clearly caused by the steric hindrance between C16–H and C22–H. Despite the lack of planarity, some limited forms of π-conjugation may be occurring between the pyrazine and 4-methoxyphenyl rings due to the C1–C11 and C2–C21 bond distances (1.475(3) and 1.480(3) Å, respectively), which are a little shorter than typical C–C σ bonds (1.53 Å), and this is in agreement with a similar structure published in the literature.[12] Intermolecular packing of this molecule is based on van der Waals forces and the presence of an intermolecular π,π-stacking between the rings C21–C26 and C1–N6. The centroid–centroid distance between them is 3.684 Å.

2.3. Absorption and fluorescence properties

The UV–vis and fluorescence spectroscopic data in chloroform solution and in thin film for the 2,3-dicyanopyrazine derivatives are summarized in Table 1. In dilute solution, all the compounds exhibit two maxima absorption wavelengths peaking at around 270–310 and 350–380 nm, respectively. The highest and lowest energy absorption bands are assigned to π–π* transitions due to their high molar absorption coefficients. These compounds display blue emission in solution (λ_{em}^{max} 440–480 nm) with quantum fluorescence yields (Φ_F) from 0.003 to 0.1 and Stokes shifts of around 90 nm. The luminescence of these compounds may be attributed to π–π* fluorescence of the 2,3-dicyanopyrazine ring.

Figure 3 shows the UV–vis absorption and fluorescence spectra in solution of the intermediate compounds **8** and **10**. The presence of free hydroxyl groups in compound **10** led to a hypsochromic shift of around 10 nm in the spectra and also led to a lower quantum yield. The final compounds **11**–**16** exhibit similar absorption and fluorescence patterns in the curves (Fig. 4). Compound **13** showed a bathochromic shift of around 80 nm in the highest energy absorption band due to its additional phenyl conjugated ring, but this had no effect on the Stokes shift.

Table 1. Optical absorption and emission spectroscopic data for 2,3-dicyanopyrazine derivatives

Compd	λ_{abs}^{max}/nm[a] ($\varepsilon/10^4$)[b]	λ_{em}^{max} /nm[a,c]	Stokes shift/nm[a]	Φ_F[d]	λ_{abs}^{max}/nm[f]	λ_{em}^{max}/nm[f,c]	Stokes shift/nm[f]	E_g^{opt}/eV
8	383 (2.4) 314 (1.9)	482	99	0.101	385 317	492	107	2.99
10	372 (2.3) 305 (2.0)	470	98	0.053	388 320	—[g]	—	2.92
11	350 (2.1) 268 (4.6)	444	94	0.008	372 255	430	58	3.14
12	348 (1.9) 283 (3.2)	437	89	0.003	342	512	174	3.30
13	359[e] (2.5) 309 (5.9)	445	86	0.010	367[e] 305	456	89	3.23
14	347 (2.0) 276 (7.2)	438	91	0.007	353 273	432	79	3.25
15	347 (2.5) 282 (6.1)	438	91	0.007	347 282	498	151	3.32
16	348 (2.4) 281 (5.1)	440	92	0.005	348 280	488	140	3.28

[a] 2,3-Dicyanopyrazine derivatives of 10^{-5} M in chloroform.
[b] Units=$mol^{-1}\,cm^{-1}$.
[c] Excitation wavelength was at lowest energy maxima of absorption.
[d] Quantum yield of fluorescence using quinine sulfate in 1 M H_2SO_4 as standard (Φ_F=0.546).
[e] Shoulder peak.
[f] In solid thin film.
[g] Diphenol **10** is not fluorescent in solid state.

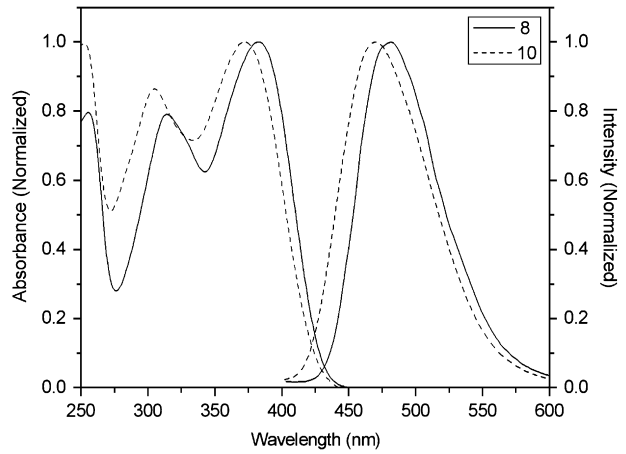

Figure 3. Normalized absorption and fluorescence spectra in chloroform solution for compounds **8** and **10**.

Compounds **11**–**16** also present fluorescence in the solid state. Optical absorption and emission of these materials in the solid state were measured in thin films, obtained by spin coating from chloroform solution onto a quartz plate.

The solid state optical absorption and emission spectra of compounds **11**–**16** are shown in Figure 5. The lowest energy absorption bands relating to the 2,3-dicyanopyrazine ring, observed in solution, are also seen in the solid state. The solid state optical absorption bands are, however, red shifted for most of the compounds, as in **11**, **13**, and **14**, showing an increase of 22, 8, and 6 nm, respectively, compared to the corresponding bands in solution. This may be due to a slight increase in planarity in the solid state leading to an increase in the conjugation.[13] On the other hand, **12** exhibits a blue shift of 6 nm in the lowest energy absorption band in the solid state, and **15** and **16** do not show changes in the spectra. The optical band gaps (E_g) of all compounds were determined by their corresponding absorption in thin films, using the same method applied in the literature[14] (Table 1). The optical band gap varies from 2.92 eV in **10** to 3.32 eV in **15**. The E_g wavelengths were obtained from the derivative of the UV curves, giving the midpoint between the threshold energy at which the lowest energy absorption band starts increasing and that at which it starts decreasing (Supplementary data).

Thin films of **11**, **13**, and **14** exhibit blue fluorescence (Fig. 5b). Of these compounds only **13**, containing a biphenyl

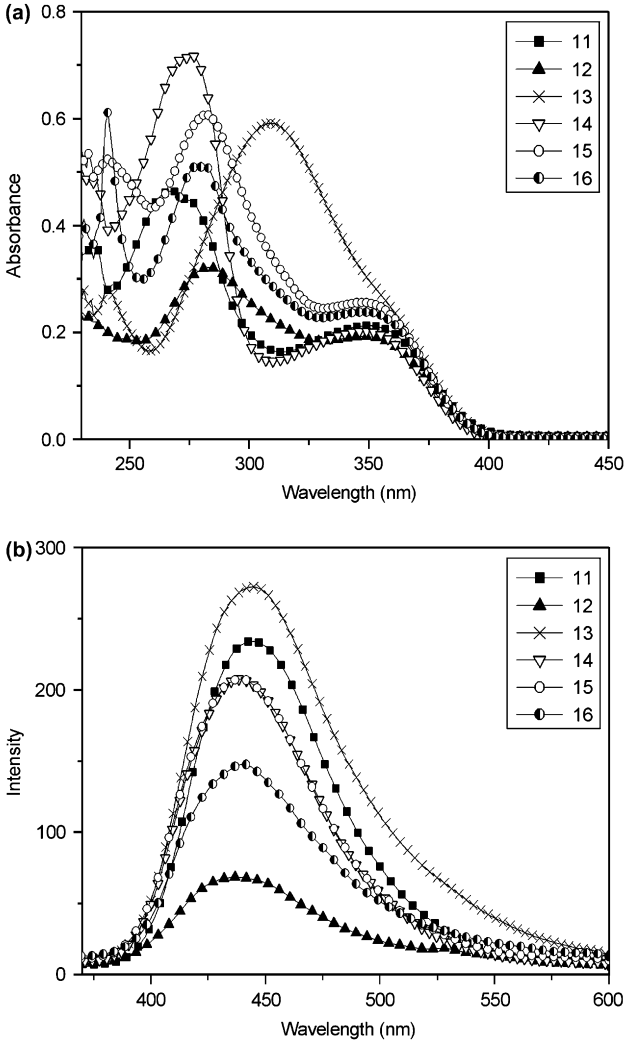

Figure 4. Optical absorption (a) and fluorescence (b) spectra of **11**–**16** in chloroform solution.

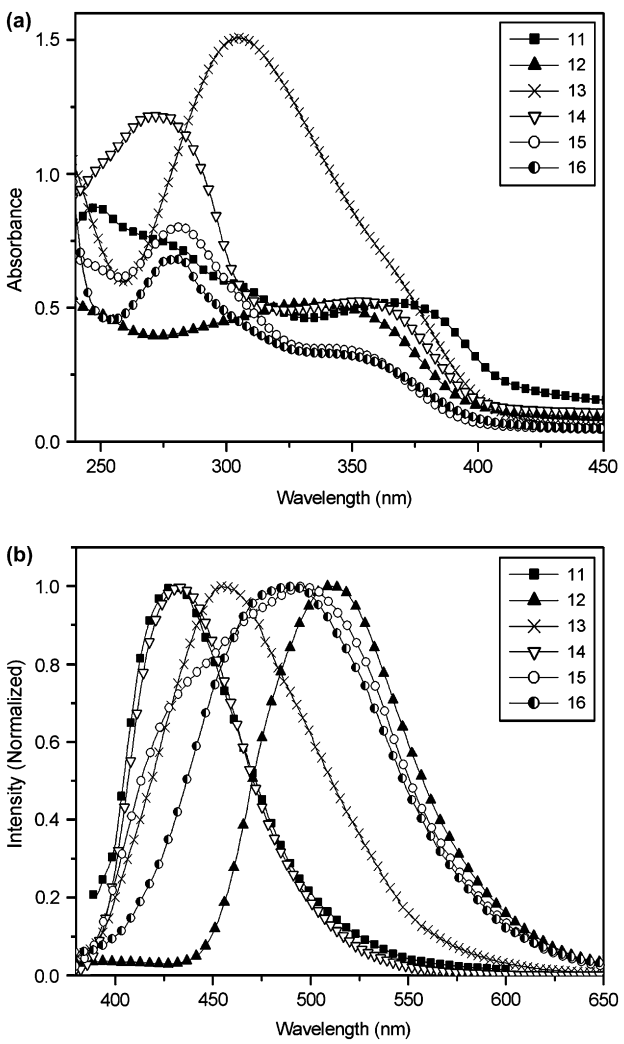

Figure 5. Optical absorption (a) and fluorescence (b) spectra of **11**–**16** in solid state.

unit, shows a red shift (11 nm), as **11** and **14** show a slight blue shift (14 and 6 nm, respectively) relative to their emission in chloroform solution. However, for bulky compounds containing more alkyl chains, such as **12**, **15**, and **16**, the fluorescence is strongly red shifted from 50 to 75 nm compared to that observed in solution, with large Stokes shifts (174, 151, and 140 nm, respectively). These compounds exhibit a green emission in solid state. A broadening in the fluorescence spectra is also observed for these compounds, especially for **15**.

2.4. Thermal properties

The thermal behavior of **11–16** was investigated by DSC, optical microscopy, and thermogravimetry, and the results are summarized in Table 2. Some of the materials (**11**, **12**, and **15**) exhibit a glassy state on the second heating after melting, with no or little crystallization on cooling the isotropic liquid. On heating sample **11** there are two crystal–crystal transitions at 56 and 97 °C, and the material melts at 114 °C to an isotropic liquid. On cooling, no crystallization is observed, even when the material is allowed to stand for over a week. A second heating gives only a glass transition at 87 °C. Compound **12** has a similar profile, exhibiting only a glass transition at a lower temperature (6.2 °C) on a second heating of the sample.

Compounds **13**, **14**, and **16** show partial crystallization on cooling of the isotropic liquid. On cooling, a monotropic smectic C phase is observed just before the crystallization of compound **13**, detected only by optical microscopic analysis. This may be taken as evidence for a certain degree of order in this material, due to the possibility of intermolecular packing by van der Waals forces and intermolecular π,π-stacking, which are observed in the X-ray analysis of the central core (intermediate **8**, see Section 4.3). Compound **14** shows partial crystallization on cooling of the isotropic liquid, being in a semi-crystalline state. On a second heating, the sample starts to recrystallize at around 97 °C and then melts at 135 °C. No glass transition temperature was observed. Compound **15** is a wax that does not have a melting point, exhibiting only a glass transition temperature at 32 °C.

Table 2. Thermal properties of compounds **11–16**

Compd	Transitions	T (ΔH)[a] heating	T ($-\Delta H$)[a] cooling	T_g[a]	T_{dec}[b]
11	Cr–Cr′	56 (8.13)	—	87	416
	Cr′–Cr″	97 (13.5)	—		
	Cr″–I	114 (37.3)	—		
12	Cr–Cr′	19 (2.62)	—	6.2	431
	Cr′–I	52 (40.1)	—		
13[c]	Cr–I	171 (38.1)	147 (36.2)	—	411
14	SCr–Cr	97 (−26.0)		—	425
	Cr–Cr′		100 (13.4)		
	Cr′–I	135 (61.2)	112 (16.1)		
15	g–I	—	—	32	434
16	Cr–I	93 (16.7)	76 (15.4)	—	295

[a] Determined by DSC 10 °C/min.
[b] By TGA, onset of decomposition in nitrogen, 10 °C/min.
[c] Optical microscopy shows monotropic smectic C. *Cr=crystal, SCr=semi-crystalline state, I=isotropic liquid, g=glassy state.*

The thermal stability was analyzed by TGA. In most cases the onset of decomposition is in the range of 410–430 °C, showing a good thermal stability for electro-optic device applications. Compound **16**, containing semi-flexible benzyl units, shows a lower thermal stability, decomposition starting at 295 °C.

2.5. AFM of thin films

Spin-coated films of **14** and **15** showed quite diverse superficial structures, in topographic images obtained from atomic force microscopy (AFM) (Fig. 6). Both the films presented a homogeneous deposition on the glass substrate, however, the surface of the film of compound **14** had a morphology with grain boundaries typical of crystallized layers, consistent with a more crystalline structure, also confirmed previously by DSC measurements. On the other hand, the

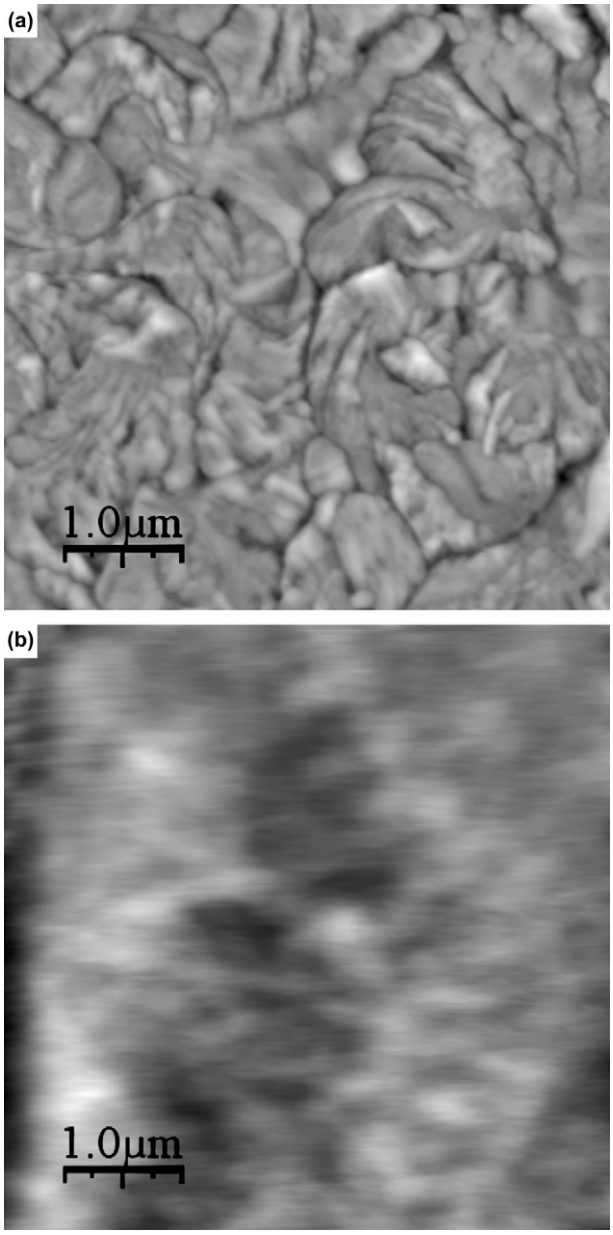

Figure 6. AFM images showing the surface morphology of solid films of **14** (a) and **15** (b).

topography of the film of compound **15** is similar to that of amorphous systems. This trend is in agreement with the differences observed in their luminescent and thermal properties. From the AFM images, we obtained the superficial roughness of the films, which is around 16 nm for **14** and 7 nm for **15**, indicating that the film of sample **15** is flatter.

3. Conclusions

In summary, a series of luminescent V-shaped low molecular mass materials containing a 2,3-dicyanopyrazine central core were synthesized and characterized. The photophysical and thermal properties of these compounds, in solution and in solid state, were evaluated. These compounds displayed fluorescence in the solid state in a wide range of the spectra (from 430 to 512 nm). Most of the materials achieved good thermal stability, exhibiting an amorphous glassy state after melting. Consequently, fluorescent transparent amorphous films can be easily obtained from these compounds by spin coating.

4. Experimental

4.1. General

Infrared spectra were recorded on a Perkin–Elmer model 283 spectrometer in KBr discs or films. ^{1}H NMR spectra were obtained with a Varian Mercury Plus 400-MHz instrument using tetramethylsilane (TMS) as the internal standard. ^{13}C NMR spectra were recorded on a Varian Mercury Plus 100-MHz spectrometer. Elemental analyses were carried out using a Perkin–Elmer model 2400 instrument. Low-resolution mass spectra were recorded on a triple quadrupole mass spectrometer, GCMS-QP5050A Shimadzu. The melting points, thermal transitions, and mesomorphic textures were determined using an Olympus BX50 microscope equipped with a Mettler Toledo FP-82 hot stage and a PM-30 exposure control unit. DSC measurements were carried out using Shimadzu equipment with a DSC-50 module. An HP UV–Vis model 8453 spectrophotometer was used to record absorption spectra. Fluorescence spectra were recorded on a Hitachi-F-4500. The relative quantum yields of fluorescence (Φ_F) for all compounds are determined according to Eq. 1:

$$\Phi_{unk} = \Phi_{std}(I_{unk}/A_{unk})(A_{std}/I_{std})(\eta_{std}/\eta_{unk})^2 \quad (1)$$

where Φ_{std} is the fluorescence yield of standard quinine sulfate (Φ_{std}=0.546 in 1 M H_2SO_4 at 298 K); I_{unk} and I_{std} are the integrated emission intensities of the sample and standard, respectively; A_{unk} and A_{std} are the absorbance of the sample and standard, respectively, at the desired wavelength λ_{exc} (380 nm) such that absorbances were less than 0.10; and η_{unk} and η_{std} are the refractive indexes of the sample and standard solutions.

4.2. Materials

All the reagents were obtained from commercial sources and used without further purification. In general, all the compounds were purified by column chromatography on silica gel (70–230 mesh), and crystallization from analytical grade solvents. Carboxylic acids **1**, **2**, **3**, and **4** were prepared according to published procedures.[15–18] 4′-(3,4,5-Tridodecyloxybenzoyloxy)benzoic acid **5** was obtained from the iterative esterification of 3,4,5-tridodecyloxybenzoic acid **2** with benzyl-4-hydroxybenzoate followed by deprotection of the benzyl ester through a modified version of a procedure given in the literature.[19] Acid **6** was synthesized through Williamson etherification of methyl 3,4,5-trihydroxybenzoate with 4-*n*-dodecyloxybenzyl bromide, followed by alkaline ester cleavage according to a method described in detail elsewhere.[20] Anisil **7** was synthesized through benzoin condensation of anisaldehyde[21] followed by hydroxyl oxidation using copper(II) sulfate/pyridine.[22] Compound **9** was synthesized according to a procedure given in the literature.[22]

4.3. X-ray crystallographic analysis

Suitable crystals of **8** were obtained through recrystallization from methanol followed by filtration of the crystals and washing with cold methanol. Crystallographic analysis was carried out at room temperature with a selected prismatic yellow crystal, which was mounted on a CAD-4 Enraf–Nonius diffractometer using graphite monochromated Mo Kα radiation (λ=0.71073 Å). Cell parameters were determined from 25 centered reflections in the θ range of 4.96°–16.99°. Intensities of 3130 were collected using the $\omega-2\theta$ scan technique with a θ angle ranging from 1.65 to 25.07°. The structure was solved using direct methods with SIR-97[23] and refined by full-matrix least-squares procedures on F^2 using SHELXL-97.[24] H atoms bonded to C atoms were added at their calculated positions and included in the structure factor calculations, with C–H distances and U_{eq} taken from the default of the refinement program. Selected crystal data: $C_{20}H_{14}N_4O_2$, M=342.35, monoclinic, $P2_1/n$, a=9.498(1) Å, b=7.38(1) Å, c=24.664(2) Å, β=93.72(1)°, V=1726.0(3) Å^3, Z=4, D_{calcd}=1.317 Mg/m^3, μ=0.089 mm^{-1}, F(000)=712, unique 3056 (R_{int}=0.0147), refined parameters=237, Goof (F^2)=1.032, $R_1[I>2\sigma(I)]$=0.0422, wR_2 (all data)=0.1207.

Crystallographic data (excluding structure factors) for the structure reported in this paper have been deposited at the Cambridge Crystallographic Data Centre under supplementary publication number CCDC 623033. Copies of the data can be obtained, free of charge, on application to CCDC, 12 Union Road, Cambridge, CB2 1EZ, UK [fax: +44(0) 1223 336033, e-mail: deposit@ccdc.cam.ac.uk or http://www.ccdc.cam.ac.uk)].

4.4. Film preparation and characterization

The films were deposited on quartz plates for the optical absorption and emission measurements. Before deposition, the plates were first carefully cleaned by washing with neutral detergent and then, followed by a sequence of 20-min sonications in acetone, alcohol, and water, and finally dried in an oven. The studied compounds were dissolved in chloroform, at 2% (wt), and then deposited by spin coating at 4000 rpm for 30 s, at room temperature (24 °C).

The quality of solid films obtained from samples **14** and **15** was observed with an atomic force microscope (AFM), using MI (Molecular Imaging Model IC 301) in contact mode, at a 2.60 Hz scanning rate and 256×256 lines.

4.5. Synthesis of 2,3-dicyanopyrazine ring

A mixture of compound **7** or **9** (10 mmol), diaminomaleonitrile (1.3 g, 12 mmol), and catalytic amount of *p*-toluenesulfonic acid in methanol (20 mL) was heated under reflux overnight. After cooling, the precipitate was filtered and washed with cold methanol to give the crude product as a yellow powder.

4.5.1. 2,3-Dicyano-5,6-bis(4-methoxyphenyl)pyrazine (8). The solid was recrystallized from acetonitrile. Yield: 85%; mp 190.2–190.6 °C. IR (KBr pellet) ν_{max} cm^{-1}: 2967, 2838, 2233 (C≡N), 1603, 1504, 1376, 1260, 1175, 1024, 840. ^1H NMR ($CDCl_3$) δ ppm: 3.85 (s, 6H, CH_3O), 6.87 (d, J=6.8 Hz, 4H, Ar–H), 7.54 (d, J=6.8 Hz, 4H, Ar–H). ^{13}C NMR ($CDCl_3$) δ ppm: 55.7, 113.7, 114.5, 127.9, 128.9, 131.7, 154.5, 162.2. Elemental analysis for $C_{20}H_{14}N_4O_2$, calcd: C, 70.17; H, 4.12; N, 16.37. Found: C, 69.89; H, 4.15; N, 16.18%.

4.5.2. 2,3-Dicyano-5,6-bis(4-hydroxyphenyl)pyrazine (10). The crude product was purified by column chromatography (eluant hexane/ethyl acetate 1:1). Yield: 78%; mp 185 °C (dec). IR (KBr pellet) ν_{max} cm^{-1}: 3407 (OH), 2250 (C≡N), 2213, 1607, 1590, 1497, 1373, 1274, 1173, 1106. ^1H NMR ($CDCl_3$) δ ppm: 6.86 (d, J=8.8 Hz, 4H, Ar–H), 7.50 (d, J=8.8 Hz, 4H, Ar–H), 9.10 (s, 2H, ArO–H). ^{13}C NMR ($CDCl_3$) δ ppm: 114.3, 115.7, 127.6, 129.0, 131.9, 154.8, 160.2. Elemental analysis for $C_{18}H_{10}N_4O_2$, calcd: C, 68.79; H, 3.21; N, 17.83. Found: C, 68.70; H, 3.45; N, 17.49%. MS (EI, 70 eV) *m/z* (%): [M^+] 314 (88%), [M^++1] 315 (19%), [M^++2] 316 (2%), [M^+−1] 313 (49%), 297 (28%), 119 (100%).

4.6. Esterification procedure for final compounds 11–13

The corresponding carboxylic acid **1**, **2**, or **3** (2 mmol) and thionyl chloride (0.19 mL, 2.6 mmol) in dichloromethane (20 mL) were heated under reflux for 4 h. The solvent and excess of thionyl chloride were evaporated under vacuum affording the acid chloride, which was used without further purification. To a three-necked round bottomed flask with argon inlet–outlet containing compound **10** (0.314 g, 1 mmol) dissolved in dichloromethane (30 mL) and triethylamine (5 mL), the respective acid chloride in 5 mL of dichloromethane was added dropwise. The reaction mixture was then stirred at room temperature for 20 h. The solvents were evaporated to give the crude products.

4.6.1. 2,3-Dicyano-5,6-bis-4-(4-decyloxybenzoyloxy)-phenyl pyrazine (11). The crude product was recrystallized from acetonitrile as a light yellow powder. Yield: 89%; mp 113.6–115.0 °C. IR (KBr pellet) ν_{max} cm^{-1}: 2918, 2850, 2240 (C≡N, weak), 1736 (C═O), 1602, 1507, 1377, 1256, 1202, 1159, 1058. ^1H NMR ($CDCl_3$) δ ppm: 0.88 (t, 9H, $-CH_3$), 1.28–1.47 (br, 28H, $-CH_2-$), 1.82 (m, 4H, $-CH_2CH_2O-$), 4.04 (t, 4H, $-CH_2O-$), 6.97 (d, J=8.8 Hz, 4H, Ar–H), 7.28 (d, J=8.8 Hz, 4H overlapped with $CDCl_3$ signal, Ar–H), 7.67 (d, J=8.8 Hz, 4H, Ar–H), 8.12 (d, J=8.8 Hz, 4H, Ar–H). ^{13}C NMR ($CDCl_3$) δ ppm: 14.1, 22.6, 25.9, 29.1, 29.3, 29.4, 29.6, 31.9, 68.4, 113.1, 114.4, 120.8, 122.5, 129.7, 131.2, 132.3, 132.4, 153.6, 154.3, 163.9, 164.3. Elemental analysis for $C_{52}H_{58}N_4O_6$, calcd: C, 74.79; H, 7.00; N, 6.71. Found: C, 74.33; H, 7.04; N, 6.60%.

4.6.2. 2,3-Dicyano-5,6-bis-4-(3,4,5-tridodecyloxybenzoyloxy)phenyl pyrazine (12). The crude product was purified by column chromatography (eluant dichloromethane) to give a yellow wax. Yield: 67%; mp 52.5–55.4 °C. IR (film) ν_{max} cm^{-1}: 2920, 2854, 1724 (C═O), 1591, 1504, 1433, 1331, 1179, 1111, 945. ^1H NMR ($CDCl_3$) δ ppm: 0.87 (m, 18H, $-CH_3$), 1.25–1.48 (br, 108H, $-CH_2-$), 1.81–1.85 (m, 12H, $-CH_2CH_2O-$), 4.02–4.08 (m, 12H, $-CH_2O-$), 7.27 (d, J=8.4 Hz, 4H overlapped with $CDCl_3$ signal, Ar–H), 7.38 (s, 4H, Ar–H), 7.68 (d, J=8.4 Hz, 4H, Ar–H). ^{13}C NMR ($CDCl_3$) δ ppm: 14.4, 22.9, 26.3, 29.5, 29.6, 29.9, 30.6, 32.2, 69.5, 73.9, 108.8, 113.3, 122.8, 123.4, 129.9, 131.5, 132.7, 143.5, 153.2, 153.7, 154.5, 164.7. Elemental analysis for $C_{104}H_{162}N_4O_{10}$, calcd: C, 76.71; H, 10.03; N, 3.44. Found: C, 76.24; H, 10.35; N, 3.22%.

4.6.3. 2,3-Dicyano-5,6-bis-4-(4-decyloxy-4-phenylbenzoyloxy)phenyl pyrazine (13). The crude product was purified by heating in acetonitrile (40 mL) and the solid filtered off as a light yellow powder. Yield: 70%; mp 170.0–172.5 °C. IR (film) ν_{max} cm^{-1}: 2921, 2851, 1734 (C═O), 1600, 1501, 1377, 1266, 1186, 1063, 825. ^1H NMR ($CDCl_3$) δ ppm: 0.89 (t, 6H, CH_3), 1.28–1.48 (br, 28H, $-CH_2-$), 1.81–1.85 (m, 4H, $-CH_2CH_2O-$), 4.02 (t, 4H, $-CH_2O-$), 7.00 (d, J=8.4 Hz, 4H, Ar–H), 7.29 (d, J=8.4 Hz, 4H, Ar–H), 7.59 (d, J=8.4 Hz, 4H, Ar–H), 7.70 (d, J=8.0 Hz, 8H, Ar–H), 8.22 (d, J=8.4 Hz, 4H, Ar–H). ^{13}C NMR ($CDCl_3$) δ ppm: 14.4, 22.9, 26.3, 29.5, 29.6, 29.7, 29.8, 32.1, 68.4, 113.3, 115.2, 122.8, 126.9, 127.0, 128.6, 129.9, 131.0, 131.5, 131.9, 132.6, 146.6, 153.7, 154.5, 159.9, 164.7. Elemental analysis for $C_{64}H_{66}N_4O_6$, calcd: C, 77.86; H, 6.74; N, 5.68. Found: C, 77.48; H, 6.80; N, 5.43%.

4.7. Esterification procedure for final compounds 14–16

A mixture of **10** (0.314 g, 1 mmol), the corresponding carboxylic acid **4**, **5**, or **6** (2 mmol), DCC (0.494 g, 2.4 mmol), and a catalytic amount of DMAP in dichloromethane (40 mL) was stirred at room temperature under argon atmosphere for 24 h. The resulting precipitate was filtered off and washed with dichloromethane (50 mL). The solvent was evaporated and the crude product was purified by column chromatography (eluant dichloromethane).

4.7.1. 2,3-Dicyano-5,6-bis-4-[4-(4-decyloxybenzoyloxy)-benzoyloxy]phenyl pyrazine (14). White solid. Yield: 74%, mp 134.3–136.7 °C. IR (film) ν_{max} cm^{-1}: 2924, 2852, 2375 (C≡N, weak), 1736 (C═O), 1602, 1508, 1376, 1260, 1202, 1160, 1052. ^1H NMR ($CDCl_3$) δ ppm: 0.89 (t, 6H, CH_3), 1.28–1.48 (br, 28H, $-CH_2-$), 1.79–1.86 (m, 4H, $-CH_2CH_2O-$), 4.05 (t, 4H, $-CH_2O-$), 6.99 (d, J=8.4 Hz, 4H, Ar–H), 7.32 (d, J=8.4 Hz, 4H, Ar–H), 7.38 (d, J=8.4 Hz, 4H, Ar–H), 7.70 (d, J=8.4 Hz, 4H, Ar–H), 8.15 (d, J=8.4 Hz, 4H, Ar–H), 8.27 (d, J=8.4 Hz, 4H, Ar–H). ^{13}C NMR ($CDCl_3$) δ ppm: 14.4, 22.9, 26.2, 29.3, 29.5, 29.6, 29.8, 32.1, 68.6, 113.3, 114.6, 121.0, 122.5, 122.7,

122.8, 126.4, 130.0, 131.5, 132.1, 132.6, 132.7, 153.5, 154.5, 155.9, 164.1, 164.5. Elemental analysis for $C_{66}H_{66}N_4O_{10}$, calcd: C, 73.72; H, 6.19; N, 5.21. Found: C, 73.67; H, 6.19; N, 5.09%.

4.7.2. 2,3-Dicyano-5,6-bis-4-[4-(3,4,5-tridodecyloxybenzoyloxy)benzoyloxy]phenyl pyrazine (15). Yellow solid. Yield: 70%; T_g 32 °C. IR (film) ν_{max} cm^{-1}: 2923, 2853, 2358 (C≡N, weak), 1737 (C═O), 1594, 1502, 1462, 1431, 1380, 1335, 1261, 1164, 1061. ^1H NMR ($CDCl_3$) δ ppm: 0.88 (m, 18H, CH_3), 1.26–1.49 (broad, 108H, –CH_2–), 1.75–1.86 (m, 12H, C$H_2$$CH_2O$–), 4.05 (t, 12H, –$CH_2O$–), 7.32 (d, J=8.4 Hz, 4H, Ar–H), 7.37 (d, J=8.8 Hz, 4H, Ar–H), 7.41 (s, 4H, Ar–H), 7.70 (d, J=8.8 Hz, 4H, Ar–H), 8.28 (d, J=8.4 Hz, 4H, Ar–H). ^{13}C NMR ($CDCl_3$) δ ppm: 14.4, 22.9, 26.3, 29.5, 29.6, 29.9, 30.0, 30.6, 32.1, 69.5, 73.9, 108.8, 113.3, 122.5, 122.7, 123.4, 126.6, 130.0, 131.6, 132.2, 132.8, 143.6, 153.3, 153.5, 154.5, 155.8, 164.0, 164.7. Elemental analysis for $C_{118}H_{170}N_4O_{14}$, calcd: C, 75.84; H, 9.17; N, 3.00. Found: C, 75.78; H, 9.11; N, 3.09%.

4.7.3. 2,3-Dicyano-5,6-bis-4-[3,4,5-tris-(4-dodecyloxybenzyloxy)benzoyloxy]phenyl pyrazine (16). Yellow solid. Yield: 59%; mp 92.9–96.0 °C. IR (film) ν_{max} cm^{-1}: 2923, 2856, 1721 (C═O), 1593, 1508, 1464, 1428, 1380, 1244, 1183, 1111. ^1H NMR ($CDCl_3$) δ ppm: 0.88 (m, 18H, CH_3), 1.26–1.44 (br, 108H, –CH_2–), 1.78 (br, 12H, C$H_2$$CH_2O$–), 3.92–3.96 (m, 12H, –$CH_2O$–), 5.04 and 5.07 (2 s, 12H, ArCH_2O–), 6.76 (d, J=8.4 Hz, 4H, Ar–H), 6.89 (d, J=8.4 Hz, 8H, Ar–H), 7.25–7.28 (m, 8H overlapped with $CDCl_3$ signal, Ar–H), 7.33 (d, J=8.4 Hz, 8H, Ar–H), 7.49 (s, 4H, Ar–H), 7.68 (d, J=8.4 Hz, 4H, Ar–H). ^{13}C NMR ($CDCl_3$) δ ppm: 14.4, 22.9, 26.3, 29.6, 29.7, 29.9, 32.1, 68.3, 71.4, 75.0, 110.0, 113.3, 114.4, 114.7, 114.9, 122.8, 123.7, 128.5, 129.5, 130.2, 130.5, 131.5, 132.7, 143.7, 153.0, 153.6, 154.5, 159.3, 164.5. Elemental analysis for $C_{146}H_{198}N_4O_{16}$, calcd: C, 77.41; H, 8.81; N, 2.47. Found: C, 76.93; H, 9.05; N, 2.16%.

Acknowledgements

The authors thank Dr. Frank Quina from Universidade de São Paulo (USP) and Dr. Faruk Nome from Universidade Federal de Santa Catarina (UFSC) for the free access to the photophysical equipment, the Laboratório de Sistemas Nanoestruturados (LabSiN) for the film deposition, and to the Laboratório de Filmes Finos e Superfícies (LFFS) for the AFM facilities, both located at Departamento de Física, UFSC. The authors thank Dr. André A. Pasa for helpful discussions. This work was supported by Conselho Nacional de Desenvolvimento Científico e Tecnológico (CNPq, Brazil), FAPESC (Brazil), FINEP (Brazil), and Merck (Germany).

Supplementary data

The complete set of the ^1H and ^{13}C NMR, UV–vis and fluorescence spectra in solid phase, as well as DSC and TGA curves of the new compounds are available. Supplementary data associated with this article can be found in the online version, at doi:10.1016/j.tet.2007.01.045.

References and notes

1. (a) Shirota, Y. *J. Mater. Chem.* **2000**, *10*, 1–25; (b) Yao, Y.-S.; Xiao, J.; Wang, X.-S.; Deng, Z.-B.; Zhang, B.-W. *Adv. Funct. Mater.* **2006**, *16*, 709–718; (c) Neto, B. A. D.; Lopes, A. S. A.; Ebeling, G.; Gonçalves, R. S.; Costam, V. E. U.; Quina, F. H.; Dupont, J. *Tetrahedron* **2005**, *61*, 10975–10982; (d) Han, M.; Lee, S.; Jung, J.; Park, K.-M.; Kwon, S.-K.; Ko, J.; Lee, P. H.; Kang, Y. *Tetrahedron* **2006**, *62*, 9769–9777; (e) Chan, L.-H.; Lee, Y.-D.; Chen, C.-T. *Tetrahedron* **2006**, *62*, 9541–9547.
2. (a) Valverde-Aguilar, G. *Opt. Mater.* **2006**, *28*, 1209–1215; (b) Serwadczak, M.; Kucharski, S. *J. Sol.-Gel Sci. Technol.* **2006**, *37*, 57–62.
3. (a) Talarico, M.; Golemme, A. *Nat. Mater.* **2006**, *5*, 185–188.
4. (a) Irie, M. *Chem. Rev.* **2000**, *100*, 1685–1716; (b) Pu, S.; Yang, T.; Xu, J.; Chen, B. *Tetrahedron Lett.* **2006**, *47*, 6473–6477.
5. Mustroph, H.; Stollenwerk, M.; Bressau, V. *Angew. Chem., Int. Ed.* **2006**, *45*, 2016–2035.
6. (a) Cristiano, R.; Ely, F.; Gallardo, H. *Liq. Cryst.* **2005**, *32*, 15–25; (b) Gimenez, R.; Piñol, M.; Serrano, J. L. *Chem. Mater.* **2004**, *16*, 1377–1383.
7. Shirota, Y. *J. Mater. Chem.* **2005**, *15*, 75–93.
8. (a) Jaung, J. Y.; Lee, B. H. *Dyes Pigments* **2003**, *59*, 135–142.
9. Kin, J. H.; Shin, S. R.; Matsuoka, M.; Fukunish, K. *Dyes Pigments* **1999**, *41*, 183–191.
10. (a) Cristiano, R.; Vieira, A. A.; Ely, F.; Gallardo, H. *Liq. Cryst.* **2006**, *33*, 381–390; (b) Cristiano, R.; Santos, D. M. P. O.; Gallardo, H. *Liq. Cryst.* **2005**, *32*, 7–14.
11. Yelamaggad, C. V.; Shashikala, I.; Rao, D. S. S.; Prasad, S. K. *Liq. Cryst.* **2004**, *31*, 1027–1036.
12. Donzello, M. P.; Ou, Z.; Monacelli, F.; Ricciardi, G.; Rizzoli, C.; Ercolani, C.; Kadish, K. M. *Inorg. Chem.* **2004**, *43*, 8626–8636.
13. Tonzola, C. J.; Alam, M. M.; Kaminsky, W.; Jenekhe, S. A. *J. Am. Chem. Soc.* **2003**, *125*, 13548–13558.
14. Joshi, A.; Manasreh, M. O.; Davis, E. A.; Weaver, B. D. *Appl. Phys. Lett.* **2006**, *89* 111907-1–111907-3.
15. Merlo, A. A.; Braun, J. E.; Vasconcelos, U. B.; Ely, F.; Gallardo, H. *Liq. Cryst.* **2000**, *27*, 657–660.
16. Hersmis, M. C.; Spiering, A. J. H.; Waterval, R. J. M.; Meuldijk, J.; Vekemans, J. A. J. M.; Hulshof, H. A. *Org. Process Res. Dev.* **2001**, *5*, 54–60.
17. Ely, F.; Conte, G.; Merlo, A. A.; Gallardo, H. *Liq. Cryst.* **2004**, *31*, 1413–1425.
18. Murthy, H. N. S.; Sadashiva, B. K. *Liq. Cryst.* **2004**, *31*, 1347–1356.
19. Lehmann, M.; Gearba, R. I.; Koch, M. H. J.; Ivanov, D. A. *Chem. Mater.* **2004**, *16*, 374–376. With modifications: DMAP was used instead of DMPS. For benzyl deprotection 1,4-dioxane was used as the solvent and the reaction temperature was 40 °C.
20. Percec, V.; Schlueter, D.; Kwon, Y. K.; Blackwell, J.; Moller, M.; Slangen, P. J. *Macromolecules* **1995**, *28*, 8807–8818.
21. Sumrell, G.; Stevens, J. I.; Goheen, G. E. *J. Org. Chem.* **1957**, 39–41.
22. Gilman, H.; Broadbent, H. S. *J. Am. Chem. Soc.* **1948**, *70*, 2619–2621.
23. Altomare, A.; Burla, M. C.; Camalli, M.; Cascarano, G. L.; Giacovazzo, C.; Guagliardi, A.; Moliterni, A. G. G.; Polidori, G.; Spagna, R. *J. Appl. Crystallogr.* **1999**, *32*, 115–119.
24. Sheldrick, G. M. *SHELXL-97, Program for Crystal Structures Analysis*; University of Göttingen: Gottingen, Germany, 1997.